Fusion Engineering and Design 86 (2011) 2557–2560

Contents lists available at ScienceDirect

Fusion Engineering and Design

journal homepage: www.elsevier.com/locate/fusengdes

Surface composition and morphology changes of JET tiles under plasma interactions

L.C. Alves[a,b], E. Alves[a,b,*], N.P. Barradas[a,b], M. Dias[a,c], R. Mateus[c], P. Carvalho[c], J.P. Coad[d], A.M. Widdowson[d], J. Likonen[e], S. Koivuranta[e], JET-EFDA Contributors

[a] Instituto Tecnológico e Nuclear, E.N. 10, Sacavém 2686-953, Portugal
[b] Centro de Física Nuclear da Universidade de Lisboa, Av. Prof. Gama Pinto 2, Lisboa, Portugal
[c] Associação Euratom/IST, Instituto de Plasmas e Fusão Nuclear, Laboratório Associado, Av. Rovisco Pais, 1049-001 Lisboa, Portugal
[d] Euratom/CCFE Fusion Association, Culham Science Centre, OX14 3DB, UK
[e] Association Euratom-TEKES, VTT, PO Box 1000, 02044 VTT, Espoo, Finland

ARTICLE INFO

Article history:
Available online 4 May 2011

PACS:
82.80.Yc
89.30.Jj
28.52.Fa

Keywords:
Ion beam analysis
Carbon fibre composites tiles
Fusion reactor materials

ABSTRACT

Plasma interactions with the main chamber of magnetic fusion devices result in net erosion from some areas and net deposition at other locations. However, high energy particle irradiation means that there are continuous erosion and re-deposition processes involved, creating new surface structures. Although the net deposition can be readily assessed, net erosion and material mixing is difficult to determine. In 2005 marker tiles were mounted in the JET vessel which have a thin tungsten (W) layer deposited on the CFC substrate with a ~10 μm carbon layer on top. This layered structure was designed to determine the areas where some erosion had occurred during JET plasma operations, when the tiles were removed for analysis in 2007.

This paper describes the results from a set of tiles mounted in a poloidal limiter (in Octant 8) at the outer wall of the main chamber; a comparison is made between the data from tiles near the top, middle and bottom of the limiter. A set of ion beam techniques together with electron microscopy were used to provide a detailed analysis of the tiles. In general, since plasma interaction is strongest near the centre of the limiter where the tile is closest to the boundary of the confined plasma, erosion dominated on the central tiles, with deposition further from the plasma boundary. Also the amount of retained deuterium is higher in the tiles located in the upper and lower regions of the plasma chamber.

© 2011 Elsevier B.V. All rights reserved.

1. Introduction

The energy scenario for the future must consider the nuclear energy as an important resource if the reduction of greenhouse gas emissions will stay as a worldwide goal. While fission reactors are based on mature technologies the fusion reactor are still under development and the success of the first prototype, the International Thermonuclear Experimental Reactor (ITER), will be crucial for the future of fusion energy [1]. Among the several problems that materials in the fusion reactor will face are the high mechanical, thermal and magnetic loads [2,3] and high irradiation fluxes. The irradiation effects are particularly important in plasma facing components (PFC) which are exposed to extreme working conditions during the lifetime of fusion reactor. Even in normal plasma conditions the materials used in these components stand very high particle fluxes and heat loads.

A major concern with plasma facing materials is the erosion due to sputtering, vaporization and chemical effects. The free atoms can be ionized and contaminate the plasma being transported by the magnetic fields inside the chamber. The contaminants that acquire enough energy leave the plasma and can be deposited with fuel elements in different parts of the chamber walls. This process leads to the formation of mixed layer at the surfaces which could enhance fuel retention and morphology changes reducing the lifetime of the reactor.

Understanding these processes and the material transport mechanisms are important for predicting the lifetime of components for future devices such as ITER. To learn more about the plasma interaction with the wall, ion beam techniques are well suited allowing a quantitative analysis of the erosion/re-deposition processes [4–6]. In previous work we studied tiles placed in the middle of the JET chamber and divertor [6]. In this work we present and discuss the results obtained from JET tiles from the outer

* Corresponding author at: Instituto Tecnológico e Nuclear, E.N. 10, Sacavém 2686-953, Portugal. Tel.: +351 219946086.
E-mail address: ealves@itn.pt (E. Alves).

0920-3796/$ – see front matter © 2011 Elsevier B.V. All rights reserved.
doi:10.1016/j.fusengdes.2011.03.093

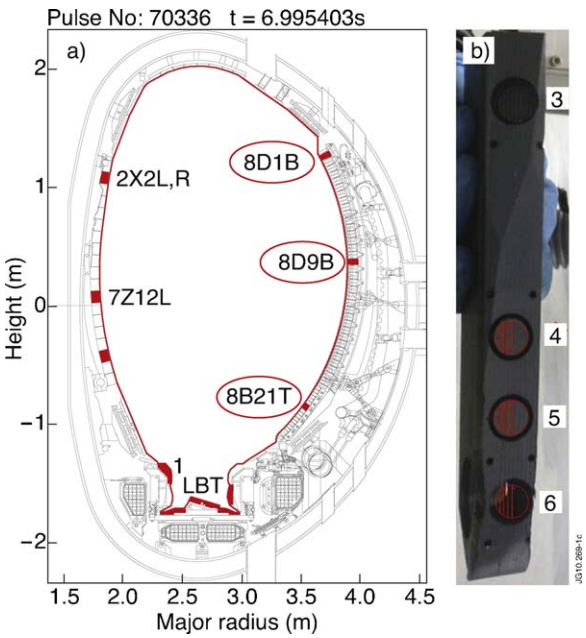

Fig. 1. Schematic of the JET reactor showing the location of the analysed carbon tiles. One of the analysed samples is also shown in the figure depicting the core numbers.

poloidal limiter (located in the upper and lower part of the chamber) exposed to deuterium plasma, combining a set of ion beam techniques (RBS, EBS, NRA, μPIXE and ERDA) with scanning electron microscopy (SEM).

2. Experimental details

The samples studied were cut from tiles removed from the JET after the 2005–2007 campaign. A cross-section of JET chamber is shown in Fig. 1 indicating the location of the analysed tiles. Tiles 8D1B and 8B21T, from the top and bottom of the chamber were studied and the results compared with tile 8D9B from the middle region already studied [6]. The samples were cut along each tile in order to obtain representative results of the composition over the entire surface. The carbon-fibre composite (CFC) tiles were coated with a thin W marker layer (about 0.2 μm) and then coated with about 10 μm of C to quantify the erosion and re-deposition processes. This procedure is well established and described in previous papers (see Ref. [5] and reference therein).

Post mortem analyses of the tiles was performed to study the composition and elemental distribution combining a set of ion beam techniques, Rutherford Backscattering Spectrometry (RBS), Elastic Beam Spectrometry (EBS), Nuclear Reaction Analysis (NRA), Particle Induce X-ray Emission (PIXE) and Elastic Recoil Detection Analysis (ERDA). A 2.0 MeV $^4He^+$ beam was used to perform RBS and ERDA while for μPIXE/RBS we used a 2.0 MeV $^1H^+$. ERDA was used to monitor the near surface concentration of ^1H and ^2H, while ^2H concentration down to ~7 μm was evaluated through NRA using a 2 MeV and 2.3 MeV $^3He^+$ beam and the $^2H(^3He,p)\alpha$ reaction [7]. Using a 2.3–2.5 MeV $^1H^+$ beam EBS analysis allowed the determination of the Be content as well as its profile distribution up to 15 μm in depth, while allowing also evaluation of the ^2H content. The data were analysed with the NDF code including pile-up and double scattering effects [8,9]. ERDA cross-sections were calculated with SigmaCalc 1.6 by A. F. Gurbich (http://www-nds.iaea.org/sigmacalc/). The ERDA experiments probe only a fairly shallow region of the sample, about one order of magnitude less than the RBS spectra. The surface and cross-section topography of all the samples were studied by SEM with a field emission gun JEOL JSM-7001F instrument, equipped for EDS and EBSD analyses.

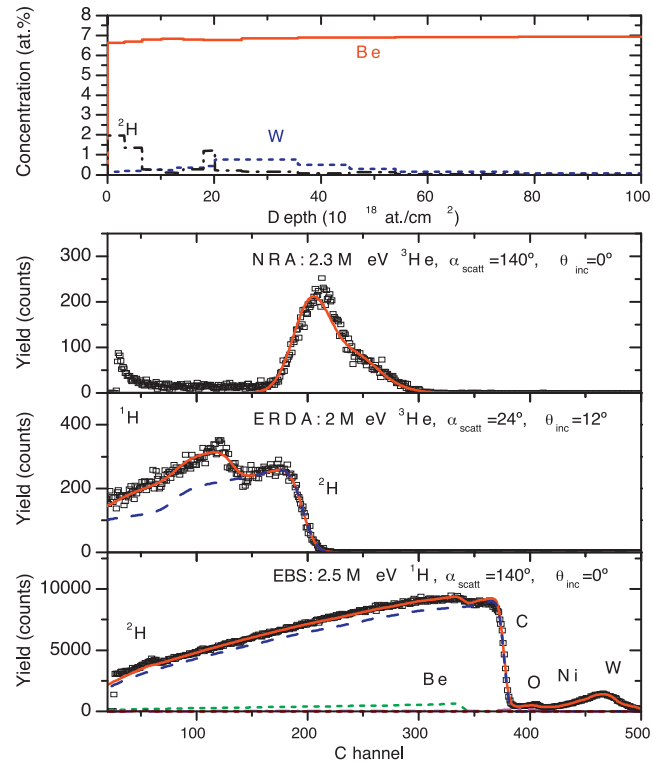

Fig. 2. IBA spectra obtained from OPL sample 8B21T-6: (bottom) 2.45 MeV H^+ beam EBS spectrum, identifying not only the presence of W, Ni, and O, but also of Be and ^2H; (middle) 2 MeV $^4He^+$ beam ERDA spectrum, showing the contribution for H and ^2H and NRA of the deuterium depth profile; (top) depth profiles of the major impurities.

3. Results and discussion

The erosion re-deposition processes were followed in tiles placed at the top (8D1B) middle (8D9B) and bottom (8B21T) of the JET chamber. A detailed analysis was performed along the tiles measuring 6 cores where 4 of them are indicated in Fig. 1. The RBS results of the poloidal tiles clearly show the combined effects of erosion and co-deposition. Fig. 2 shows an example of the NRA, ERDA, EBS and RBS spectra obtained from core 6 of tile 8B21T. Apart from the presence of W and Ni, oxygen was also detected at the surface of the sample. The PIXE analyses shows trace impurities like Ti, Cr, Mn, Fe, Ni, Cu at the ppm level. Besides deuterium, the ERDA spectrum indicates high contents of hydrogen, probably adsorbed from the atmosphere. For the deuterium and using a 2.3 MeV $^3He^+$ particles we could establish a depth profile distribution down to a depth of 6–7 μm. EBS with 2.5 MeV protons allowed to determine that the altered surface layer contains an amount of Be close to 7 at%. Exploring the NDF capabilities of consistently combining all the data from the several ion beam techniques an impurity depth profile distribution can be established as shown in Fig. 2 for some elements. Furthermore the extracted profiles are continuous within the entire region probed by the ^4He ion beam (over 10 μm assuming a density of 1.6 g/cm^3 for the depth conversion).

Using the ITN nuclear microprobe, we extended our experimental possibilities adding lateral resolution and imaging. We measured the elemental distribution maps both for sample surface and sample cross-section analysis by PIXE or RBS techniques using a 2 MeV H^+ microbeam, focused down to 3 μm × 4 μm. This allowed obtaining surface topography maps of the altered surface

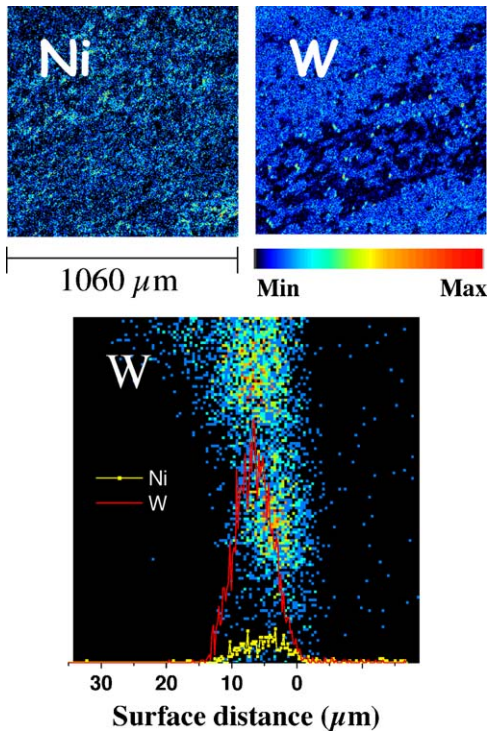

Fig. 3. (Top) Nuclear microprobe surface analysis of sample 8B21T-6, showing the Ni (left) and W (right) elemental distribution obtained. (Bottom) Sample cross-section mapping of W depicting the depth profile of Ni and W.

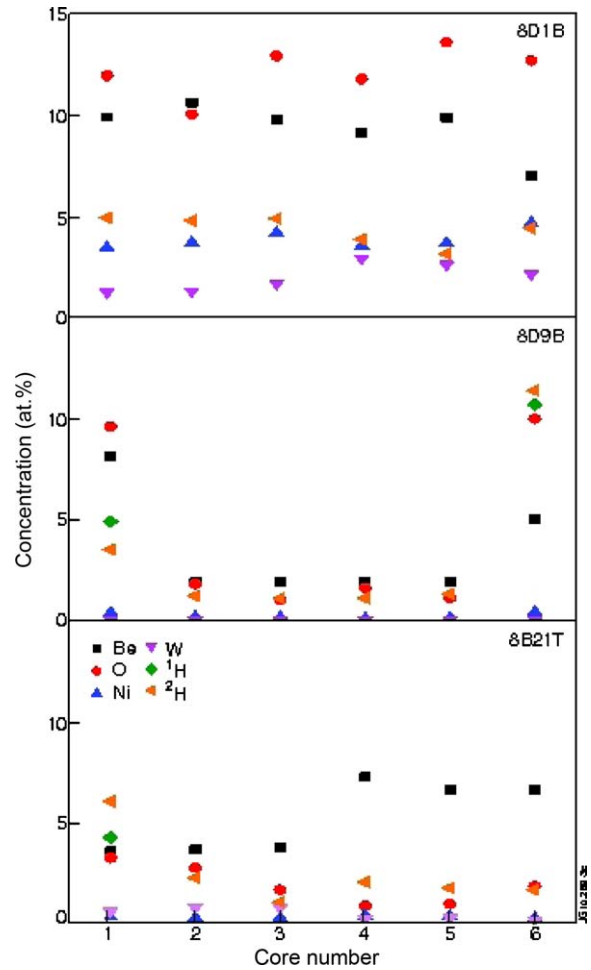

Fig. 4. Distribution of the major elements present in the cores (1–6) along the tiles. The values were obtained combining all the IBA data for each sample.

and the impurity depth distribution profiles. The results confirm that besides W and Ni, the altered surface layer contains different amounts of metallic trace elements such as Ti, Cr, Mn, Fe, Cu. Fig. 3 shows the Ni and W distribution maps at the surface of core 6 of tile 8B21T as well as the W map obtained in sample cross-section analysis. Also shown in this last map are the depth elemental distribution profiles obtained for W and Ni. The origin of the depth scale corresponds to the sample surface. The results show a complete overlap of the depth profile of the impurities present in the first 10–15 μm of the sample.

The relevant results obtained from all the cores of each tile regarding the composition are summarized in Fig. 4. The values were averaged over the first 500 nm of the samples. The accumulation of the hydrogen isotopes, Be and O in a small region at both end of the tile 8D9B and the low concentration of contaminations in the central part are consistent with an active erosion process covering nearly all the tile and a deposition or diffusion towards the tile end. Also the complete removal of the W marker layer proves the existence of a high erosion process in this region of the reactor chamber. In the upper and bottom tiles we notice a constant distribution along the tiles for most of the elements. The content of Be in these tiles is relatively high and two times higher in the upper region compared with the lower region. Also the oxygen content in upper region is much higher than in the others. This could be related with the formation of BeO, a strong exothermic oxidation reaction that needs some attention in case of an accident. The presence of a higher content of W in the upper tile suggests a lower erosion rate on that region of the chamber compared to the lower part. From the concentration distribution analysis no conclusive evidence could be established regarding the W transport in the plasma. The Be deposited in the tiles comes from the beryllium evaporated in the chamber.

The high erosion in the central region of the chamber is related with the plasma distribution at the initial stage. The plasma starts with a circular cross-section resting on the OPL, so the initial plasma interaction is with the central tiles. The interaction is more intense in the middle of the tile where some erosion is expected, whereas towards the ends of the tile where it curves away from the plasma, deposition can occur. After the plasma formation phase there is no direct contact of the OPL with the confined plasma any more, however there is still bombardment by ions travelling in the plasma boundary and from energetic neutrals which are responsible for the re-deposition and surface topography changes.

To see in more detail the surface topography, SEM images were obtained for all the samples. The results shown in Fig. 5 were obtained for core 6 of the tiles in plain view and cross-section. As referred to before, when the pulse is started the plasma interaction is with the central OPL tiles causing net erosion. We do not see the original 10 μm carbon top layer above the W layer on any of the tiles. At areas where there is generally net deposition (tiles 8B21T, 8D1B and the ends of 8D9B) a deposited layer is found on top of the W, suggesting that the carbon layer does not survive. The more central tile is clearly eroded and the W itself has also been eroded away as we have shown in our previous work [6]. From the mixed surface layers it is evident that after initial strong erosion process a subsequent re-deposition process occurs where the Ni (coming from the Inconel structural material also composed of Cr and Fe) mixes with the W marker at the surface region as shown in Fig. 3. This should be related with the plasma dynamics during the operation. The final surface layer must be formed by the re-deposition of plasma impurities during later phases of the plasma pulse. The high contents and profile distribution of ^{1}H and ^{2}H also

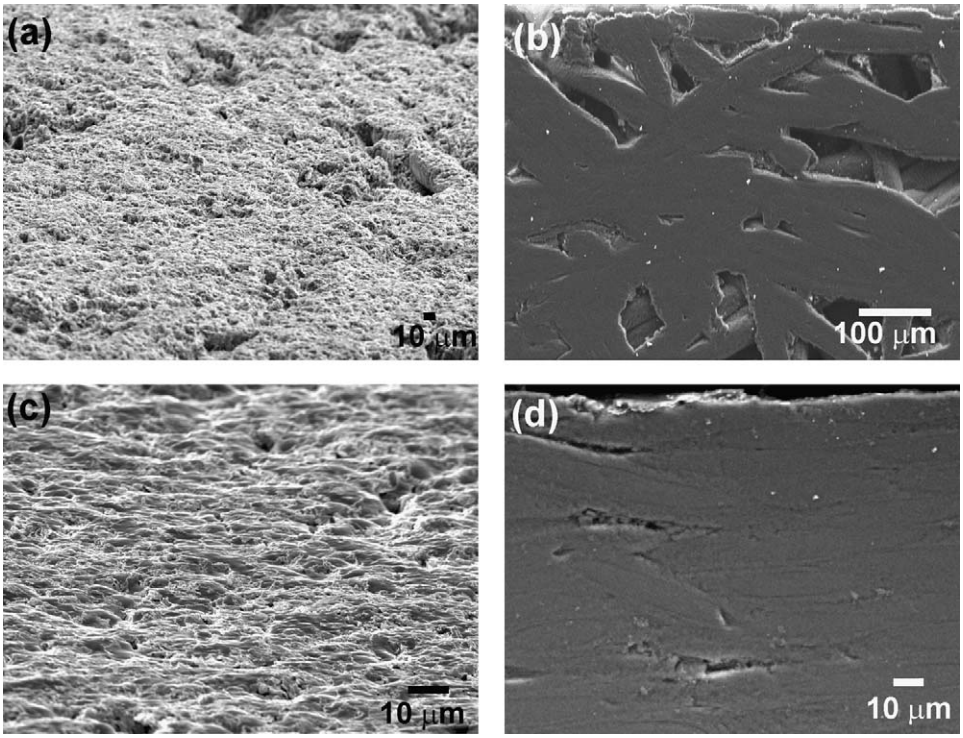

Fig. 5. Typical surface topography details of tiles 8D1B (top row) and 8B21T (bottom row) obtained by SEM analysis. The images (a) and (c) were obtained with the samples tilted 70°, and images (b) and (d) refer to samples cross-section analysis.

suggest that the fuel retention occurs during the re-deposition of the plasma impurities. Both the upper and lower tiles show a very irregular surface.

The tile 8D1B has a "porous" surface with high contents of Be and O suggesting the occurrence of a preferential chemical erosion. This open structure is a good reservoir for the hydrogen isotopes and this tile retain the highest deuterium content, around 5 at%. The lower tile 8B21T also shows a very irregular surface but without the same degree of porosity and much lower deuterium content.

4. Conclusions

Ion beam analytical techniques (RBS, EBS, ERDA and NRA) complemented with microbeam data and SEM were combined in a self-consistent mode, in order to study the erosion of the plasma facing components and re-deposition of the plasma impurities and fuel in JET OPL tiles.

The results show enhanced erosion process in the tiles placed in the middle of the chamber while the tiles at the upper and lower regions were less eroded. These findings were also observed in previous JET campaigns. The impurity profiles prove that all the original 10 μm C coating is removed and afterwards re-deposition of plasma impurities occurs. An amount of 2 at% of ^{2}H was incorporated within the re-deposited layer.

SEM images indicate that the surface of the upper tile is porous consistent with a chemical process and retains an amount of ^{2}H around 5 at%. The observed high content of Be and O in this tile could indicate the formation of BeO. The surface of the tile in the lower region of the chamber is less irregular and contains about 2 at% of ^{2}H.

Acknowledgments

This work was supported by the European Fusion Development Agreement (JW10-FT-3.59) and the software development was supported by the SPIRIT project, Grant Agreement No. 227012-CP-CSA.

References

[1] Y. Shimomura, J. Nucl. Mater. 329–333 (2004) 5–11.
[2] H. Bolt, V. Barabash, W. Krauss, J. Linke, R. Neu, S. Suzuki, N. Yoshida, J. Nucl. Mater. 329–333 (2004) 66–73.
[3] J. Roth, et al., J. Nucl. Mater. 390–391 (2009) 1.
[4] M. Rubel, J.P. Coad, D. Hole, Vacuum 78 (2005) 255.
[5] J. Coad, J. Likonen, M. Rubel, E. Vainonen-Ahlgren, D.E. Hole, T. Sajavaara, T. Renvall, G.F. Matthews, Nucl. Fusion 46 (2006) 350–366.
[6] L.C. Alves, E. Alves, N.P. Barradas, R. Mateus, J.P. Coad, A.M. Widdowson, J. Likonen, Nucl. Instrum. Methods B 268 (2010) 1991–1998.
[7] V.Kh. Alimov, M. Mayer, J. Roth, Nucl. Instrum. Methods B 234 (2005) 169–175.
[8] N.P. Barradas, M. Reis, X-Ray Spectrom. 35 (2006) 232–237.
[9] N.P. Barradas, Nucl. Instrum. Methods Phys. Res. B 225 (2004) 318–330.